Engineering Structures 86 (2015) 146–156

Contents lists available at ScienceDirect

Engineering Structures

journal homepage: www.elsevier.com/locate/engstruct

Application of PP-ECC in beam–column joint connections of rigid-framed railway bridges to reduce transverse reinforcements

Rui Zhang [a,*], Koji Matsumoto [a], Takayoshi Hirata [b], Yoshikazu Ishizeki [b], Junichiro Niwa [a]

[a] Department of Civil Engineering, Tokyo Institute of Technology, Japan
[b] Department of Construction System and Materials, Technical Research Institute Technology Division, Obayashi Corporation, Japan

ARTICLE INFO

Article history:
Received 27 May 2014
Revised 25 December 2014
Accepted 3 January 2015

Keywords:
PP-ECC
Beam–column joint
Stirrup ratio
Flexural failure
Railway bridge

ABSTRACT

In the rigid-famed railway bridges, due to extensive amount of transverse reinforcements in the joint connections, the over congestion at the connection brings the difficulties in fabricating and casting. With the objective of avoiding the congestion, Polypropylene Fiber Reinforced Engineered Cementitious Composite (PP-ECC), as one kind of Engineered Cementitious Composites, was implemented to reduce the extensive amount of transverse reinforcements in the beam–column joint connection of rigid-framed railway bridges. The basic mechanical properties of PP-ECC were confirmed by compression and uniaxial tensile tests. The effects of reducing stirrup ratio in PP-ECC beams were investigated by four-point beam tests, including two normal reinforced concrete (RC) beams and five PP-ECC beams with stirrup ratios ranging from zero to 0.42%. Having confirmed the shear reinforcing effect of PP-ECC, three one-sixth scale beam–column joint connections were constructed and tested by applying a cyclic load. A specimen was prepared following the structural design of existing railway bridges in Japan but without transverse reinforcements in the joint. Further, two more specimens were prepared with reduced stirrups and ties in the beam and column, respectively. The experimental results reveal that the PP-ECC is effective in replacing transverse reinforcements in the beam–column joints of railway rigid-framed bridges.

1. Introduction

Bridges are vital components of transportation that requires a high degree of protection to ensure their safety during a strong earthquake. The extensive damages of RC bridges observed in the past earthquakes such as Northridge, Kobe and 2011 Great East Japan earthquakes triggered extensive researches on the behavior of beam–column joint connections for designing and constructing a safer infrastructure, which further resulted in the improvements of design codes focusing on providing sufficient ductility in the vulnerable structural member to prevent its brittle failure during a major seismic event. Accordingly, for reinforced concrete (RC) structures, a considerable amount of steel reinforcements are required to be provided in these vulnerable regions, such as the plastic hinge in the beam end adjacent to the column face in a beam–column joint connection in the rigid-framed railway bridges (Fig. 1), to confine the concrete to realize the formation of ductile inelastic behavior in the plastic hinge. However, the increased and elaborated reinforcement details bring the difficulties in fabricating this complicated steel reinforcement cage as well as placing and consolidating concrete in it during the construction phase. The contradiction between increased high cost for design and construction due to these complicated reinforcements with accordingly raised requirements on seismic performance becomes more and more apparent.

Previous researches [1–6] on steel fiber reinforced concrete (SFRC) have devoted significant effort studying the behavior of joints under reversed cyclic loadings, as well as on the development of design recommendations for ensuring sufficient ductile behavior in beam–column joint connections while reducing the transverse reinforcement. SFRC, as one type of the fiber reinforced concretes (FRCs), is characterized by a tensile strain softening behavior after reaching its first cracking strength. However, a newly developed fiber-reinforced cement-based material named Engineered Cementitious Composites (ECC) exhibits multiple fine cracking, pseudo strain hardening behavior, large strain capacity between 1% and 5% and superior ductility. Its superior strain capacity makes it an ideal material for use in the plastic hinge of beam–column joint connections to undergo large inelastic deformation and reducing the quantity for transverse reinforcements. So far, various types of fibers have been utilized to produce ECCs, including steel, carbon and polymer fibers [7],

* Corresponding author at: 2-12-1-M1-17, O-okayama, Meguro-ku, Tokyo 152-8552, Japan. Tel.: +81 3 5734 2584; fax: +81 3 5734 3578.
E-mail address: zhang.r.ab@m.titech.ac.jp (R. Zhang).

http://dx.doi.org/10.1016/j.engstruct.2015.01.005
0141-0296/

Fig. 1. Rigid-framed railway bridges.

whereas most structural and retrofit applications of ECC reported in the literature use polymer fibers. The steel reinforced ECC (R/ECC) structural members such as column with reduction of shear reinforcements [8] have been confirmed in previous studies. However, the amount of previous research on applying ECC in the beam–column joints was limited and mainly focuses on the interior beam–column joints in the buildings. The previous research [9,10] have revealed the feasibility of total elimination of transverse reinforcements in the joint and increasing stirrup spacing in beam plastic hinge in beam–column joins constructed with Polyethylene Fiber Reinforced Engineered Cementitious Composites (PE-ECC).

In this research, a cementitious composite combined with fabricated polypropylene fibers (Fig. 2) named Polypropylene Fiber Reinforced Engineered Cementitious Composites (PP-ECC) with improved bond properties exhibiting the pseudo strain hardening and multiple fine cracking of ECC [11] was utilized to reduce the transverse reinforcements in beam–column joint connections of rigid-framed bridges. Compared with widely used polymer fibers such as polyvinyl alcohol (PVA) fibers or polyethylene (PE) fibers, polypropylene (PP) fiber is softer, costs lower and disperses faster, which all results in better workability. In addition, because of the hydrophobic and non-polar nature of PP fiber, PP-ECC has better durability in an alkaline environment [12]. The loading tests including two phases were conducted: a total of seven beams including five PP-ECC and two normal RC beams with varying stirrup ratios were tested to verify the shear effectiveness of PP-ECC in the first phase and a total of three one-sixth scaled T-shaped beam–column joint specimens which were prepared based on the design standards for existing railway bridges in Japan [13] were tested under the applied reversed cyclic load to verify the possibility of reducing transverse reinforcements.

2. Mechanical properties of the PP-ECC

2.1. Production of PP-ECC

The target nominal compressive strength of the PP-ECC is 30 N/mm^2. The material components and mixture proportion used in this investigation were based on a study by Hirata et al. [11]. Ordinary Portland Cement (OPC), fly ash (maximum grain size of 0.3 mm), water and 3% volume fraction of PP fibers were combined using mix proportion tabulated in Table 1. The air content of PP-ECC used in this study is around 10%. The PP fibers, as shown in Fig. 2, are fibrillated fibers having diameter of 36 μm, length of 12 mm, tensile strength of 482 MPa and elastic modulus of 5 GPa. This fibrillated polypropylene fiber with rugged surface results in improvement of bond properties and exhibits the pseudo strain hardening and multiple fine cracking of ECC under tensile stress [11]. Having finished the mixing process, the fresh PP-ECC was cast and placed into the formworks and cured for 24 h. After the removal of formwork, all of the PP-ECC specimens in this study were coated by soaked cloths to maintain the moist-curing environment for 28-day curing.

2.2. Compressive characteristics

The compressive characteristics of PP-ECC were inspected by employing the cylinder compression test. The PP-ECC cylinders with diameter of 100 mm and height of 200 mm were prepared. The compressive strengths of PP-ECC cylinders cast along with different specimens in this study are tabulated in Table 1. Different from the normal concrete in mixture, since the PP-ECC in this study uses no coarse aggregates instead of PP fibers, the average value of elastic modulus of the PP-ECC cylinders in RE-42 is 1.5×10^4 N/mm^2 which is lower than that of the normal strength concrete while the elastic modulus of the concrete with compressive strength of 29.1 N/mm^2 is 2.8×10^4 N/mm^2 in this study. However, as shown in Table 1, the compressive strength of the PP-ECC in this study is almost equivalent to that of the normal strength concrete.

2.3. Tensile characteristics

Tensile behavior, as one of the most important characteristics of ECC, was investigated by employing the uniaxial tensile method in this study. As shown in Fig. 3(a), the PP-ECC plate specimens with rectangular cross section of 76 mm wide and 13 mm thick were designed. The length of plate specimen is 200 mm, including 50 mm connecting length for attaching aluminum plates at both sides of plate. For each PP-ECC plate specimen, four aluminum plates were prepared for connecting the loading facility. The testing range of the PP-ECC plate is 100 mm. Two linear variable differential transformers (LVDTs) setting parallel to the loading direction at both sides of the plate as shown in Fig. 3(b), were used to measure the axial tensile deformation. The speed of load head was selected as 0.1 mm/min.

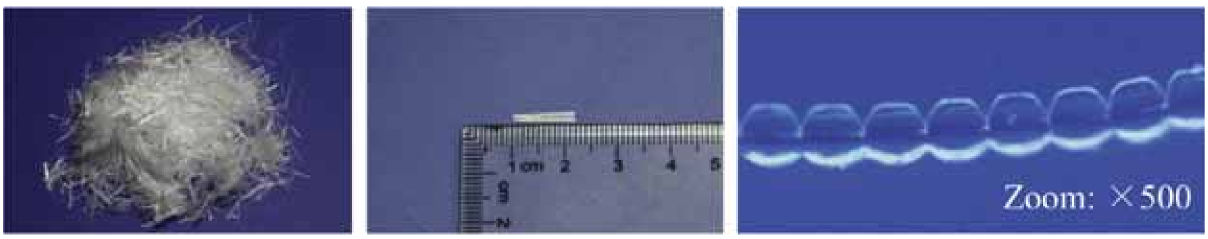

(a) A cluster of fibers. (b) Length of fiber. (c) Cross section view under a microscope.

Fig. 2. Polypropylene fiber used in this study.

Table 1
Properties of PP-ECC.

Specimen	f_{ECC} (N/mm²)	Slump flow (mm)	W/B (%)	FA/B (%)	Unit weight (kg/m³) W	B	PP fiber	AE
RE-42	30.4	Approx. 500	27	33	371	1400	27	7
RE-30	33.1							
RE-24	31.5							
RE-12	35.6							
RE-00	32.8							
TJ-1	48.2							
TJ-2	33.6							
TJ-3	33.6							

f_{ECC}: compressive strength of PP-ECC; *W*: water; *B*: binder; *FA*: fly ash; *AE*: air entrainment.

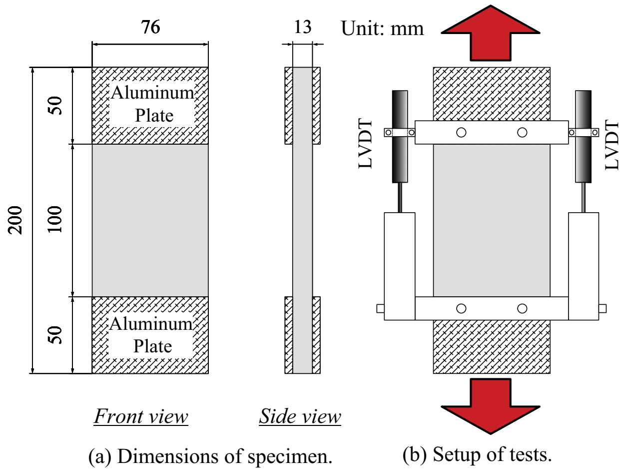

Fig. 3. Uniaxial tensile tests of PP-ECC.

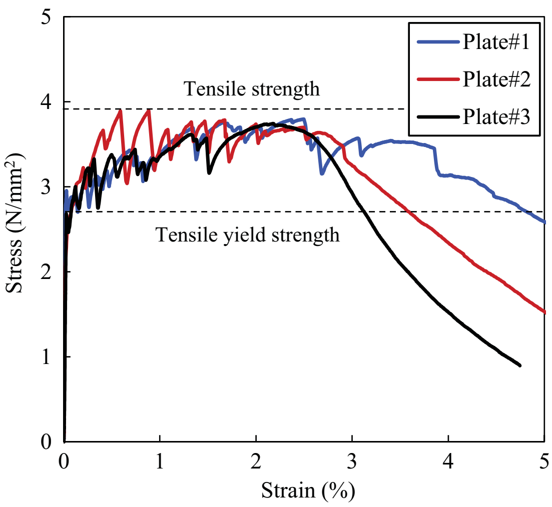

Fig. 4. Results of uniaxial tensile tests.

Tensile stress versus strain curves of the three specimens are shown in Fig. 4. The test result clearly shows typical pseudo strain hardening behavior of ECCs. From the beginning of the tests, the stress continued to increase until the first crack appeared. The stress then suddenly decreased, whereas it continued to increase after this sudden decrease as a result of the occurrence of the first crack. As the loading progressed, the increase and sudden drops of stress continued to take place accompanied by more and more fine cracks were observed on the surface of the specimen. At around 3% strain, a localized crack gradually formed and the stress began to decrease slowly. The tensile yield strength is determined as the lower value immediately after first cracking based on the stress–strain relationship. The tensile strength is defined as the maximum stress in the tensile stress–strain curve obtained from uniaxial tensile tests. In this study, the yield and tensile strength were greater than 2.5 and 3.5 N/mm², respectively.

3. Beam loading tests

3.1. Specimen layout and setup

To verify the shear effectiveness of the PP-ECC, a total of seven beams with two types of matrixes (concrete and PP-ECC), including one control beam (RC-Ref), one RC beam without stirrups within the shear span (RC-00) and five PP-ECC beams with varying stirrup ratios from the level of the control beam to zero, as summarized in Table 2, were tested. All beam specimens had the same cross-sectional dimension (150 × 300 mm), longitudinal reinforcement ratio of 2.7% and shear span-effective depth ratio of 2.8. RC-Ref was the control beam with the equivalent amount of stirrups in both shear spans symmetrically. It was designed to be failed in shear prior to the flexural failure following JSCE specification [14]. The beam corresponding to RC-Ref using PP-ECC was RE-42, having the same reinforcement arrangement as RC-Ref. In addition, a pair of beams without stirrups using concrete and PP-ECC were prepared as RC-00 and RE-00, respectively. For the remained three PP-ECC beams, the stirrup ratios varied from 0.30% to 0.12%. All stirrups were uniformly arranged within the shear span as shown in Fig. 5.

3.2. Material properties

The regular deformed steel bar with nominal diameter of 25.4 mm and yield strength of 400 N/mm² was used for longitudinal reinforcement in the tension side for all beams while a round steel bar with diameter of 6 mm and yield strength of 277 N/mm² was used for longitudinal reinforcement in the compression side. All specimens used deformed bars with nominal diameter of 6.35 mm and yield strength of 323 N/mm² as stirrups. The type and properties of all steel bars used in these seven beam specimens are summarized in Table 3.

The mix proportions of normal concrete was decided following the concrete mix design procedure described in "Standard specifications for concrete structures (Material and Construction)" [15] and is shown in Table 4. The PP-ECC used in beam tests is as described in Section 2. The mix proportions of PP-ECC with their compressive strengths in this study are summarized in Table 1. Since the PP-ECC is a kind of flowable cementitious material, the slump flow value of the PP-ECC in this study was measured to be approximately 500 mm. After the accomplishment of casting PP-

Table 2
Layout of beam specimens.

Specimen	Length (mm)	Stirrups		Longitudinal bar		Matrix type
		r_w (%)	s (mm)	A_s (mm^2)	p_w (%)	
RC-Ref	2100	0.42	100	1013.4	2.7	Concrete
RC-00		0.00	–			
RE-42		0.42	100			ECC
RE-30		0.30	140			
RE-24		0.24	175			
RE-12		0.12	350			
RE-00		0.00	–			

r_w: the stirrup ratio, $r_w = A_w/(b_w \cdot s)$; A_w: the cross-sectional area of one set of stirrups with spacing s; s: the spacing of stirrups; b_w: the width of the beam; p_w: the longitudinal reinforcement ratio, $p_w = A_s/(b_w \cdot d)$; A_s: the total cross-sectional area of longitudinal reinforcements; d: the effective depth of beam.

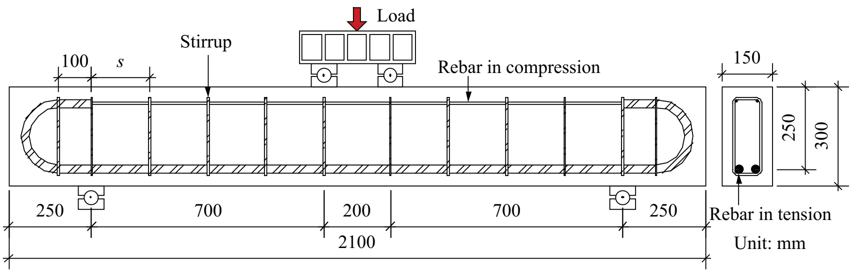

Fig. 5. Dimensions and reinforcement details of beam specimens in beam tests.

Table 3
Properties of steel reinforcements in beam tests.

Steel bars	Nominal diameter (mm)	f_y (N/mm^2)	f_u (N/mm^2)	ε_y
Rebar in tension	25.4	400	577	0.002000
Stirrup	6.35	323	499	0.001615
Rebar in compression	6.0	277	434	0.001385

f_y: the yield strength; f_u: the ultimate strength; ε_y: the yield strain.

ECC, it was poured into the formwork by moving the pouring position continuously along the direction of the beam axis.

3.3. Test results

As shown in Fig. 6, that are the failed shear spans at the ultimate stage after the loading tests, all beams were failed in shear with a localized inclined crack developed in the shear span during the loading tests. The load carried by a beam versus its midspan deflection curves for all specimens involved in this study are shown in Fig. 7. Different from the shear failure in brittle manner of RC beams, the failure process in PP-ECC beams was much gentler and the critical cracks were observed when the loading progressed exceeding to the peak loads. The shear capacities of all beams were compared by choosing the shear capacity of the control beam RC-Ref as the standard, as shown in Fig. 8. Even with a monotonic reduction in stirrup ratio from 0.42% to 0.12%, the shear capacity of PP-ECC beams still exhibited higher shear capacity than that of the control beam. As for two pairs of counterpart beams, RC-Ref and RE-42 that are beams with the same amount of stirrups, RC-00 and RE-00 that are beams without stirrups, the shear capacity of beams with and without stirrups increases 20.6% and 107.6%, respectively by using PP-ECC, which attributes to the bridging effect resulting from the PP fibers. For RC beams governed by shear failure, the shear capacity will decrease significantly with the decrease in stirrup ratio. Different from RC beams, as shown in Fig. 9, the effect from stirrup ratio is less significant in PP-ECC beams. It also appears a possibility that the PP-ECC could be a replacement of the stirrups in beam–column joint specimens.

4. Experimental program of beam–column joints

4.1. Test specimens

In the loading tests of beam–column joint specimens, an existing railway bridge designed following the Japanese code, “Design Standard for Railway Structures and Commentary (Concrete Structures)” [13], was considered as a prototype structure in this study. Since this type of rigid-framed railway bridge is stiffer in longitu-

Table 4
Properties of concrete.

Specimen	f'_c	G_{max}	W/C	Unit weight (kg/m^3)				
	(N/mm^2)	(mm)	(%)	W	C	S	G	Superplasticizer
RC-Ref	29.1	20	60	177	294	830	970	2.94
RC-00	34.9	20	60	177	294	830	970	2.94
Prototype	30.0	25	55	160	297	*	*	*
TJ-1	50.0	15	60	169	281	830	896	2.82
TJ-2	45.2	15	60	169	282	830	896	2.82

f'_c: compressive strength of concrete; W: water; C: cement; S: fine aggregate; G: coarse aggregate.
* Data not available.

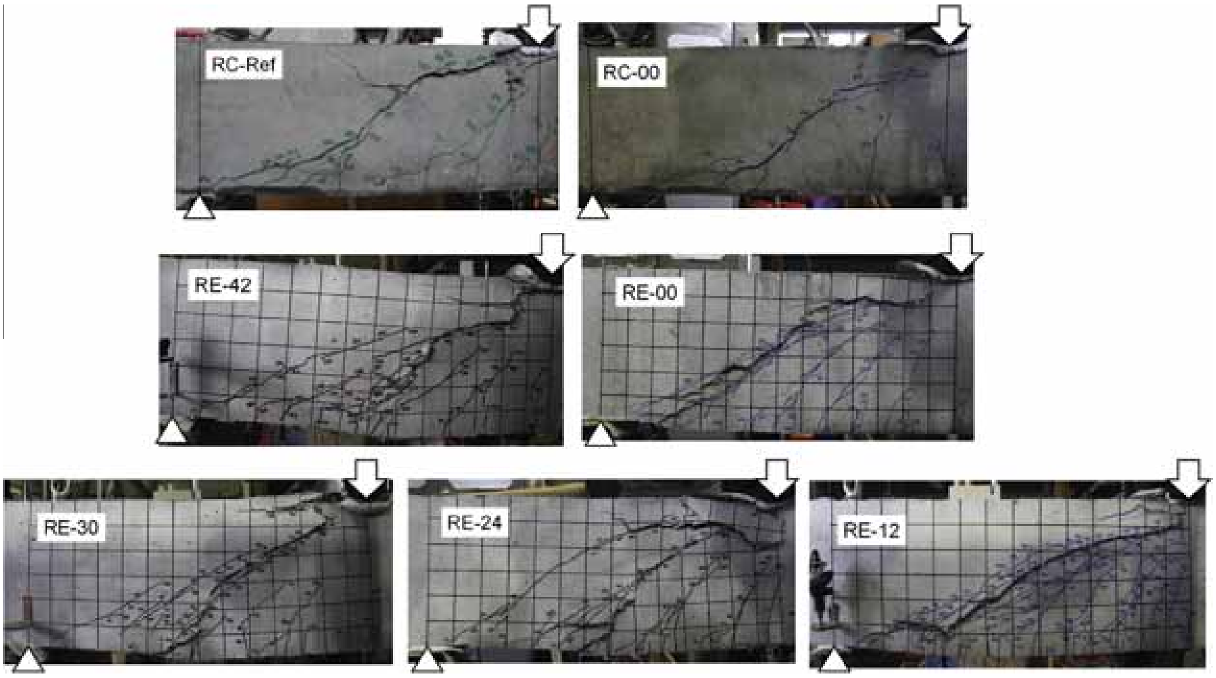

Fig. 6. Crack pattern of failed span in beam specimens after loading tests.

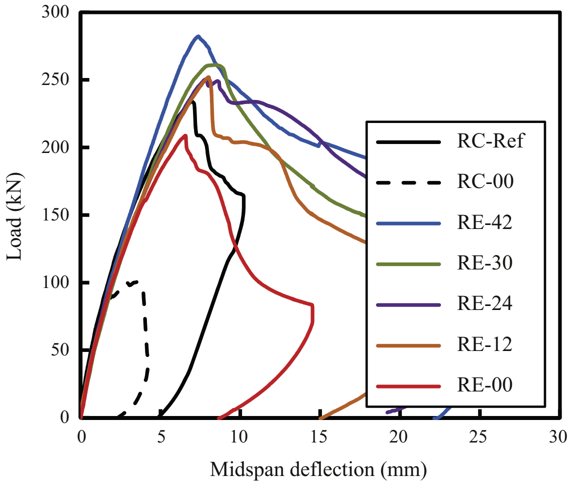

Fig. 7. Load vs. midspan deflection curves of beam tests.

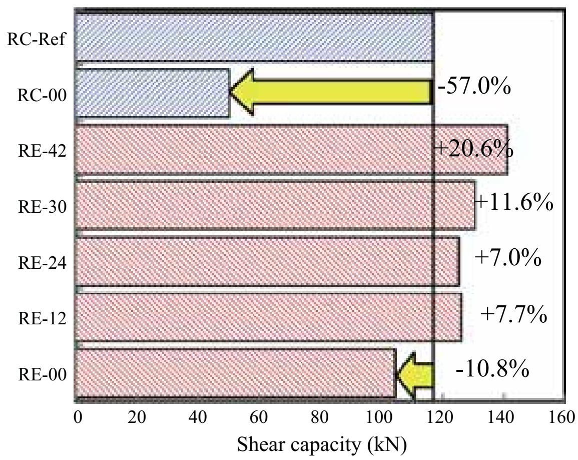

Fig. 8. Comparisons of shear capacities.

dinal direction but vulnerable in transverse direction to earthquakes, the frame structure in transverse direction was selected as the study target. Totally three specimens with different amount of transverse reinforcements were constructed on one-sixth scale, corresponding to a beam–column joint connection in the prototype bridge formed by three inflection points under an idealized laterally applied seismic load, in which two points locates at the middle points of the column section above and below the intermediate beam and another one locates at the middle point of the intermediate beam as illustrated by Fig. 10. Fig. 11(a) shows a sketch of the test setup used in this study and overall specimen details. The height of a column was considered as 1500 mm and the length of a beam from the face of a column to the end was considered as 900 mm. The column cross section was 250 mm × 250 mm, and the beam was 170 mm wide and 200 mm deep as shown in Fig. 11(b). The thickness of cover concrete was 20 mm. The transverse reinforcements in the joint were eliminated for all specimens and the amounts of longitudinal reinforcements in beams and columns were constant in these three specimens. In the specimen TJ-1, as shown in Fig. 12(a), the longitudinal and transverse reinforcements were provided in the beam and column according to the prototype bridge but without ties in the joint. Based on the specimen TJ-1, the stirrups in testing span of the beam were eliminated in the specimens TJ-2 as shown in Fig. 12(b), while the amount of longitudinal and ties in the column was kept unchanged. In the specimen TJ-3, as shown in Fig. 12(c) the amount of transverse reinforcements not only in the beam but also in the column was reduced to the minimum for fabricating a reinforcement cage. PP-ECC would be used in the beam–column joint and the beam region in TJ-1 and TJ-2 while the normal concrete would be used in the column region. However, only PP-ECC would only be used in TJ-3 specimen. The material and transverse reinforcement reductions in all specimens were summarized in Table 5. Reinforcements with nominal diameter of 6.35 mm and yield strength of 325 N/mm^2 were used for both longitudinal and transverse reinforcements in all three specimens. The mechanical properties of reinforcements as well as longitudinal and transverse

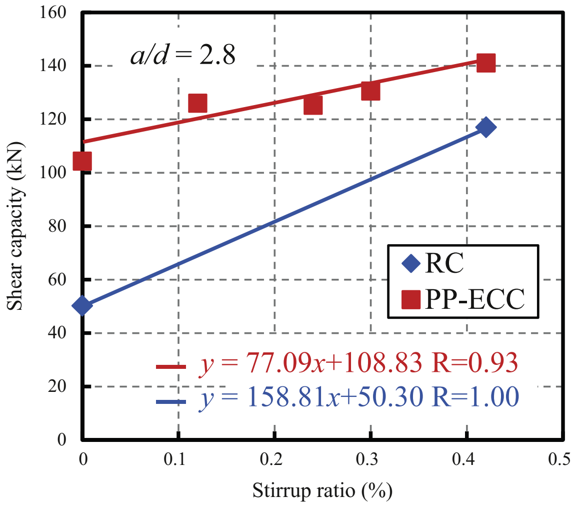

Fig. 9. Shear reinforcing effect of stirrups in RC and PP-ECC beams.

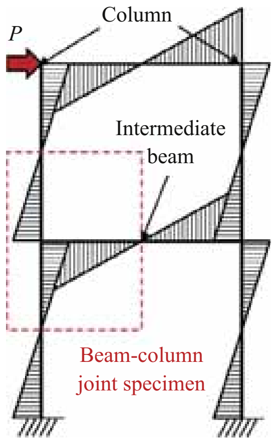

Fig. 10. Bending moment diagram under seismic force.

reinforcement ratios of the prototype bridges and specimens are summarized in Table 6. The mix proportions of normal concrete and PP-ECC used for the all beam–column joint specimens as well as their compressive strength are tabulated in Tables 1 and 4, respectively.

For the purpose of design, the strong column and weak beam concept was confirmed by calculating the ratio of the column flexural strength to that of the beam. Since there is no specific provision regarding that design concept in Japanese code "Design Standard for Railway Structures and Commentary (Concrete Structures)" [13], the relevant provision in ACI code [17] was employed to ensure that the specimens satisfy strong column and weak beam concept as shown in Eq. (1):

$$M_c/M_b \geq 1.2 \tag{1}$$

where M_c and M_b are the flexural strength of the column and the beam, respectively. The ultimate flexural strengths of the beam and the column were calculated following the JSCE code [14] for normal RC structures and the ratio of M_c to M_b was 1.67 which is greater than the value of 1.2 complying the strong column and weak beam approach. Based on the previous research [16], the replacement of normal concrete by PP-ECC in the flexural member can increase its flexural capacity around 10%. Nevertheless, M_c/M_b is still larger than 1.2.

The force equilibrium of an exterior beam–column joint is shown in Fig. 13. The total horizontal joint shear force (V_{jh}) corresponding with the flexural strength of the beam can be calculated based on Eq. (2):

$$V_{jh} = \left(\frac{H \cdot L}{H + h_c/2} \cdot \frac{1}{jd_b} - 1 \right) \cdot V_c \tag{2}$$

where V_c is the column shear force; L is the length from the beam inflection point to the column face; H is the height between upper and lower column inflection points; jd_b is the distance between the internal compression and tension force resultants in the beam which was taken as $0.9d$ and d is the effective depth of the beam; h_c is the column depth. The peak shear stress (v_j) in an exterior beam–column joint can be estimated as Eq. (3):

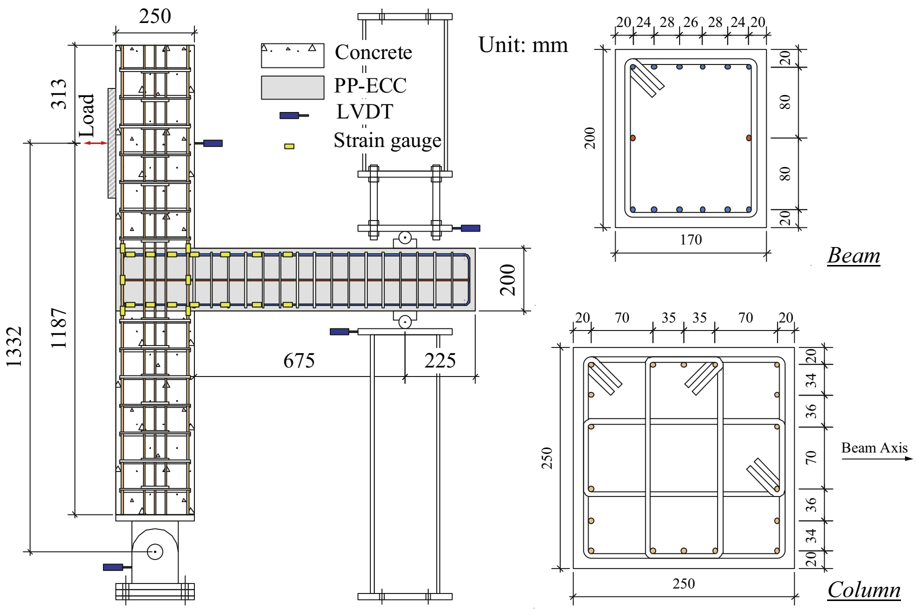

(a) Specimen dimensions (b) Cross sections of columns and beams

Fig. 11. Specimen dimensions.

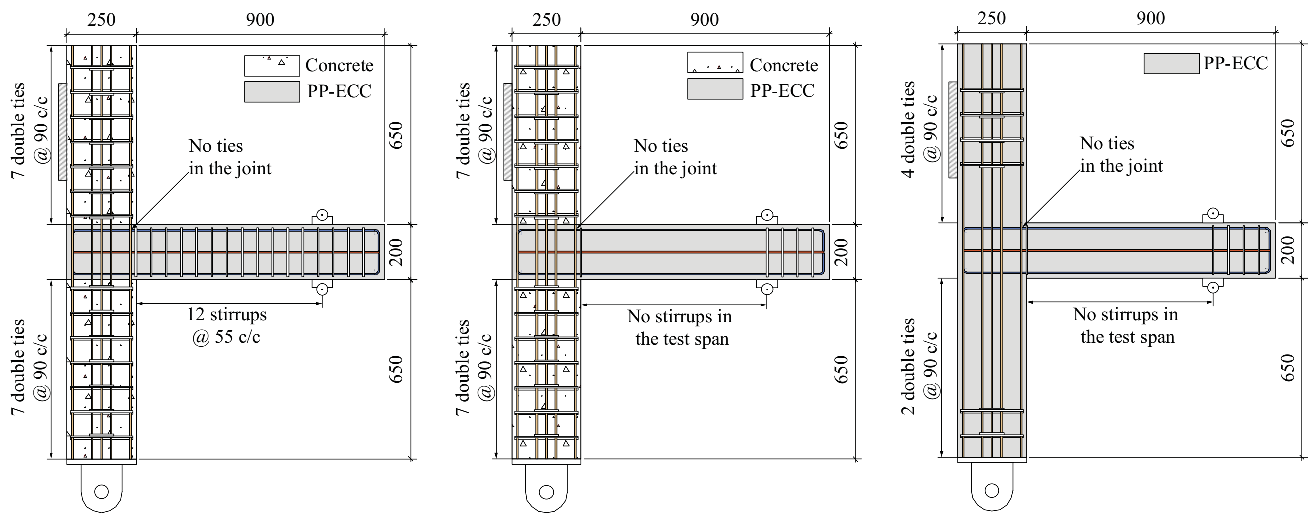

Fig. 12. Layout of specimens and reinforcement details.

Table 5
Summary of transverse reinforcement reduction.

	Transverse reinforcement ratio (%)		
	TJ-1	TJ-2	TJ-3
Joint	0	0	0
Beam	0.68	0	0
Column	0.56	0.56	0

$$v_j = \frac{M_{ub}/jd_b - V_c}{b_j h_c} \tag{3}$$

where M_{ub} is the ultimate flexural strength of the beam; b_j is the effective joint width. According to ACI Committee 318-11 [17] and the Joint ACI-ASCE Committee 352 recommendations [18], the maximum shear stress of $1.0\sqrt{f'_c}$ (MPa) is permitted in Type 2 connections with one beam framing into the column from one side.

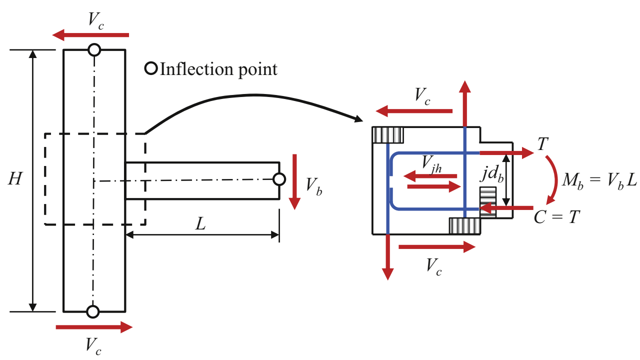

Fig. 13. Force equilibrium of an exterior beam–column joint.

4.2. Reduction in transverse reinforcements

As reported by previous studies [9,10], the use of PE-ECC can maintain adequate shear strength in the beam–column joint and beam plastic hinges without special transverse reinforcement detailing. Therefore, the ties in the joint region were eliminated for all specimens in this study. First of all loading test was conducted on TJ-1. In TJ-2 and TJ-3, transverse reinforcements in beam and column were decided to be further eliminated so that the shear capacities were closed to each other. Fig. 14 shows the reinforcements arrangement for three specimens after reducing transverse reinforcements. It was evident that more transverse reinforcements reduced, the better workability attained.

4.3. Specimen construction

For the specimen TJ-1 and TJ-2, because of two types of materials were used in one specimen, the construction sequence needs to be specially designed. As reported by the other researchers [19], since the ECC exhibits strong bonding effect to the concrete, the concrete in the column region was determined to be cast firstly. In addition, in order to increase the bonding of PP-ECC to concrete at the interface, the surface retarder, a kind of admixtures to delay the set of the surface cement paste so that the aggregate can be

Table 6
Mechanical properties and amount of steel reinforcements.

Specimen	Bar nominal diameter (mm)	Transverse reinforcement diameter (mm)	Yield strength (N/mm^2)	Tensile strength (N/mm^2)	Reinforcement ratio (%)			
					Beam		Column	
					Longitudinal reinforcement	Transverse reinforcement	Longitudinal reinforcement	Transverse reinforcement
Prototype	31.8	15.9	*	*	1.324	0.636	0.991	0.530
TJ-1	6.35	6.35	325	525	1.304	0.677	1.064	0.563
TJ-2	6.35	6.35	325	525	1.304	0.000	1.064	0.563
TJ-3	6.35	6.35	325	525	1.304	0.000	1.064	0.000

* Data not available.

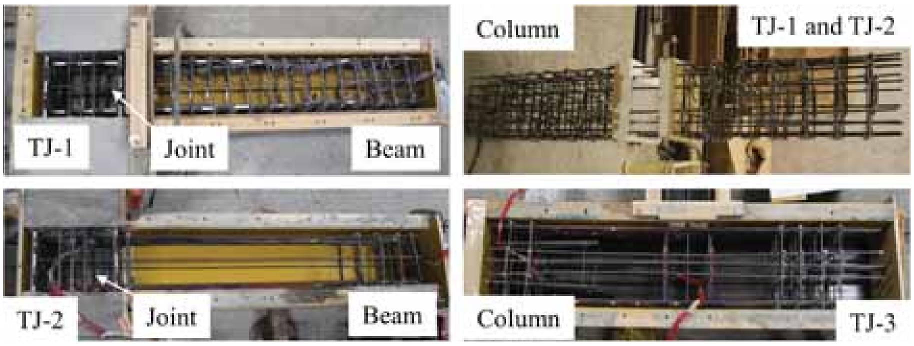

Fig. 14. Reduction of transverse reinforcements in the specimens.

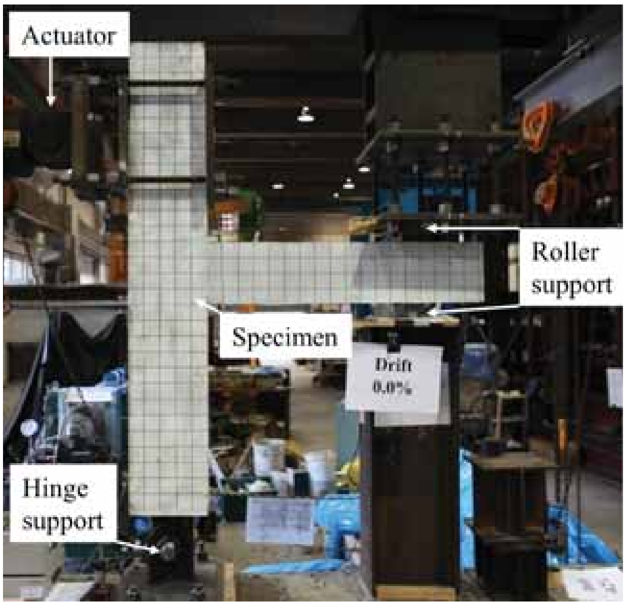

Fig. 15. Test setup.

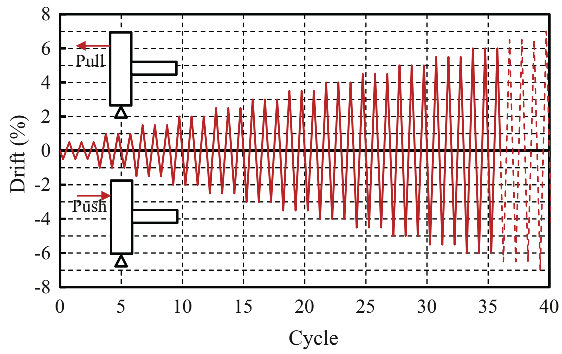

Fig. 16. Lateral displacement history.

exposed easily, was utilized. The specimen construction sequence was: firstly, the temporary formwork with surface retarder painted was set at the designed location of interface between concrete and the PP-ECC; secondly, the concrete was cast and placed into the column region; thirdly, the temporary formwork was removed after 24-h curing of concrete; fourthly, high-pressure water was utilized to flush the designed interface to expose the coarse aggregate in the concrete; PP-ECC was cast and placed into the beam–column joint and the beam region at last.

4.4. Experimental setup and procedure

All specimens were tested under a reversed cyclic load provided by a digital closed-loop controlled hydraulic loading system. The experimental setup is shown in Fig. 15. The reversed cyclic lateral displacement controlled loading was applied on the column. The bottom of the column was pinned to a strong loading frame to simulate middle height inflection point during a seismic event. At the beam length of 675 mm from the column face, two roller supports were fixed at the locations as illustrated in Fig. 11(a) to simulate middle length inflection point of intermediate link beam. The applied displacement history included 36 reversed displacement cycles ranging from 0.5% to 6.0% drift, with three cycles performed at each drift level, as shown in Fig. 16. When the column was pulled towards the actuator, the displacement was considered as positive displacement and vice versa. The drift level is defined as the ratio of the lateral displacement to the height from the hinge to the level of the applied lateral load.

5. Experimental results and discussions

5.1. Crack pattern and failure process of beam–column joint connections

Fig. 17 shows the crack patterns of all specimens observed after testing. The first fine flexural cracks initiating from the bottom edge of beams for all specimens were observed at the first cycle in the drift of 0.5%. The large number of cracks appeared before the peak loads while few cracks were developed after the peak load. The localized cracks in all specimens were noticed in the top of beam adjacent to the column face after the peak load and developed to be more and more obvious due to their opening and closing under the increased cyclic loads. In all specimens, except very limited numbers of fine flexural cracks were observed in TJ-1 and TJ-3, most of the fine flexural cracks were developed in the beam span from the column face to the roller supports and concentrated in the beam near the column face leading to the formation of flexural plastic hinge in the beam. Meanwhile, different amounts of fine inclined shear cracks were developed in the beam–column joint in all specimens. On increasing the applied drift, with opening and closing of shear cracks in the joint core region, the joint distortion and expansion continued to increase. The shear cracks adversely affected the bond between the PP-ECC and the steel reinforcements leading to the bond deterioration. Without the occurrence of localized shear cracks in all specimens, the sufficient shear strength of joints provided by PP-ECC can be developed even without tie bars in the joints, thereby allowing the formation of plastic hinges in the beams. The similarity of the failure process of TJ-1 and TJ-2 indicated that the feasibility that the PP-ECC was

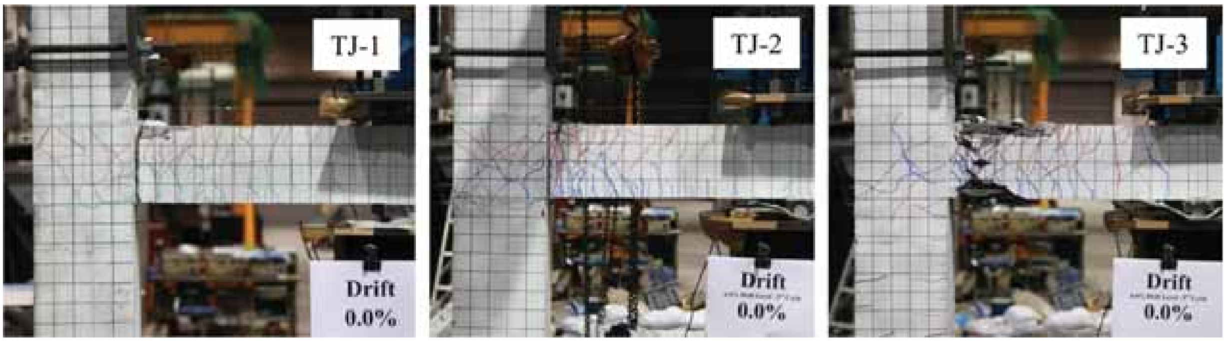

Fig. 17. Crack pattern after loading tests.

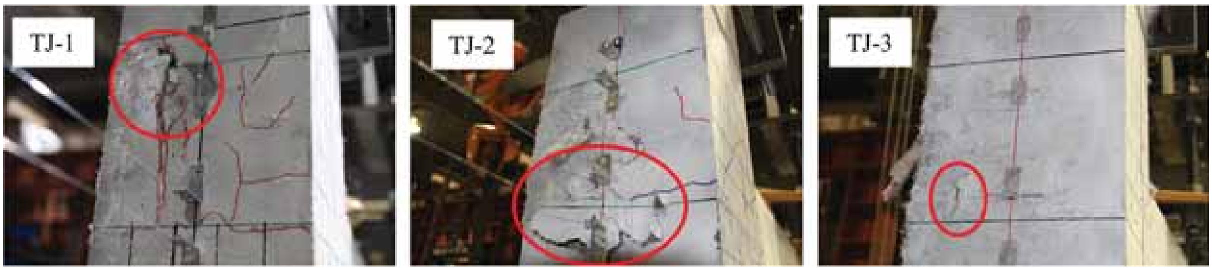

(a) TJ-1. (b) TJ-2 (c) TJ-3.

Fig. 18. Pull out of beam longitudinal reinforcements after loading tests.

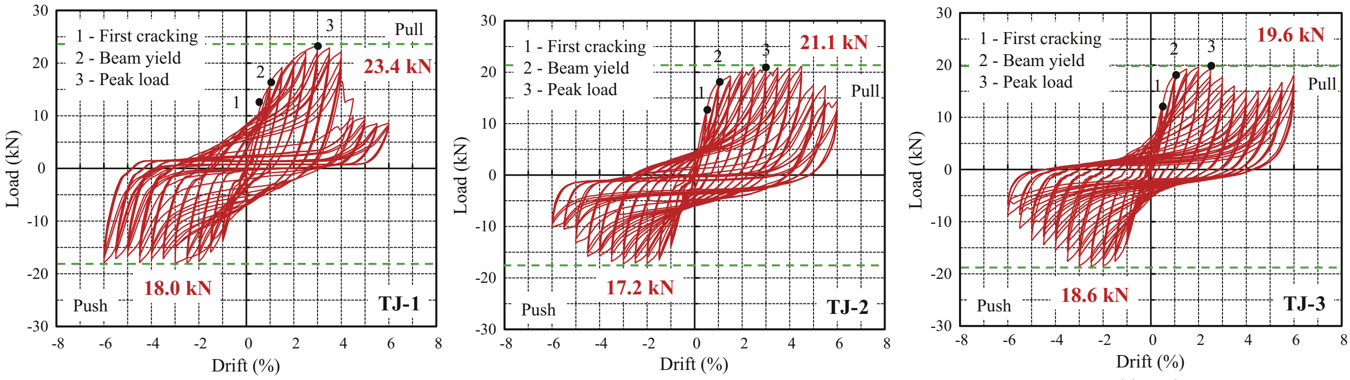

(a) TJ-1 (b) TJ-2 (c) TJ-3

Fig. 19. Load–displacement hysteretic loops.

able to be the replacement of stirrups in the beam. Different from TJ-1 and TJ-2, the crushing of partial PP-ECC with fewer fractions of PP fibers on the view side in the plastic hinge region in TJ-3 occurred at the peak load due to the inadequate distribution of PP-ECC fibers. As for the effects of this crushing, it would be discussed in the following section.

Fig. 18 shows the pull out of beam longitudinal reinforcements on the external face of a column in all specimens after the loading test due to the slipping between beam longitudinal reinforcements and the PP-ECC in the joints. Different extents of pull out of reinforcements in all specimens were observed. There were pulling out of top beam reinforcements in TJ-1 as shown in Fig. 18(a), but all beam reinforcements buckled and five out of six top beam reinforcements ruptured by the end of the loading test. The similar damage that the pull out of bottom beam reinforcements as shown in Fig. 18(b) in TJ-2 was also observed, but all top beam reinforcements buckled and only two out of six top reinforcements ruptured. The pull out of beam reinforcements in TJ-3 as shown in Fig. 18(c) was quite insignificant compared to the specimens TJ-1 and TJ-2, manifesting that the bonding between beam reinforcements and the PP-ECC in the joint of TJ-3 was the best and finally two out of six top beam reinforcements and four out of six bottom beam reinforcements ruptured. This is because the limited space between beam reinforcements and the interface in the column impaired the bonding between reinforcements and the PP-ECC.

5.2. Load–displacement hysteretic results in beam–column joint tests

The load–displacement hysteretic loops obtained from the cyclic loading tests are shown in Fig. 19. The hysteretic loops of all specimens were pinched to an equivalent level. The dashed lines with green color in each subfigure indicate the peak loads of each specimen in positive and negative loadings. The peak load of TJ-1 in positive loading cycles was the highest among all specimens, which was mainly attributed by its higher compressive strength of PP-ECC among all specimens. Fig. 20 shows the load–displacement hysteretic envelops of three specimens. It is noted from Fig. 20 that three specimens performed similarly within 2.0% drift.

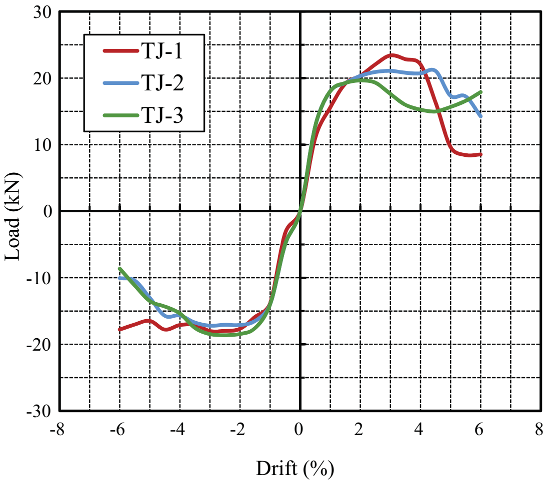

Fig. 20. Load–displacement hysteretic envelops.

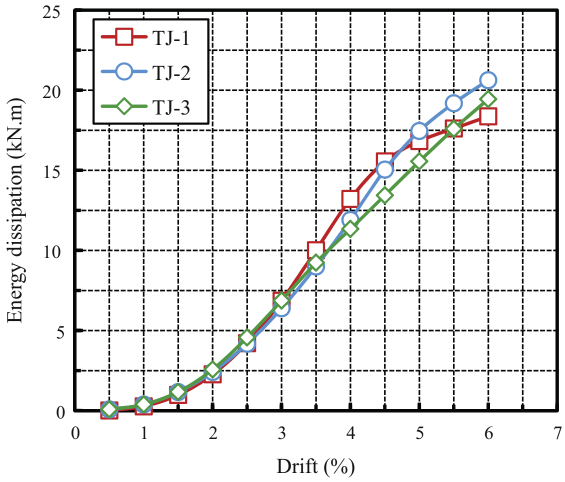

Fig. 21. Energy dissipation.

On applying the cyclic load in TJ-1 after the peak load at 3.0% drift, the load dropped drastically when TJ-1 was loaded towards 4.5% drift in the first cycle due to the ruptures of beam top longitudinal reinforcements. On reversing the load, only the beam bottom longitudinal reinforcements participated to carry the load. However, after the peak load, the strength marginally decreased in subsequent cycles up to 4.5% drift forming a plateau in load–displacement envelope curve of TJ-2 and slightly decreased from 2.5% to 4.5% but increased from 4.5% to 6.0% forming a flat basin in the load–displacement envelope curve of TJ-3 due to inelastic behavior of plastic hinge adjacent to the column face and the bond deterioration in the joint region.

Table 7 summarizes the experimental results of each specimen. The total horizontal shear force and joint stresses were calculated based on Eqs. (2) and (3), respectively. The effective joint width b_j is specified by Joint ACI-ASCE Committee 352 [18]. The peak shear stress of TJ-1, TJ-2 and TJ-3 are $0.32\sqrt{f'_c}$, $0.35\sqrt{f'_c}$ and $0.32\sqrt{f'_c}$, respectively, which are all satisfying the maximum permitted limit of $1.0\sqrt{f'_c}$ (MPa) specified by ACI code [17]. Moreover, in previous research [9], the interior beam–column joint without transverse reinforcement using ECC sustained the peak joint stress up to $1.4\sqrt{f'_c}$ (MPa), which indicates potential that ECC could be implemented in the beam–column joint subjected to a high joint stress. It is worth mentioning that the permitted joint shear stress specified by ACI code [17] was proposed based on the normal concrete structure. No design recommendations were developed to specify the permitted joint shear in the ECC beam–column joint.

5.3. Energy dissipation of beam–column joint tests

Energy dissipation indicates the capability of structures to dissipate energy through yield mechanism with satisfactory performance in the inelastic range, which occurs due to induced damages in the specimens in terms of cracking of concrete, yielding and buckling of steel reinforcements and debonding of fibers in ECC. Fig. 21 shows energy dissipation capacity of each specimen. Energy dissipation was assessed by computing the cumulative energy dissipation at each load cycle, namely, the area enclosed by the corresponding load–displacement hysterical loops. Due to the pinching and strength degradation in all specimens, the energy was not proportionally increased to the increase in the applied drift. Up to the drift of 3.0%, all specimens dissipated almost the same amount of energy. At the drift level of 4.5%, TJ-1 dissipated 15.7% more energy than the specimen without transverse reinforcements TJ-3. The growth of energy dissipation in TJ-1 slowed down markedly due to the rupture of top beam reinforcements in TJ-1 at the drift level of 4.5% while fewer ruptures of beam reinforcement in of TJ-2 and TJ-3 at this drift. As a result, the TJ-2 and TJ-3 dissipated more energy than that of TJ-1. Among all specimens, the energy dissipated by TJ-2 and TJ-3 was almost equivalent to that dissipated by TJ-1. The comparable energy dissipation even after reducing the amount of transverse reinforcements in the specimens TJ-2 and TJ-3 also highlighted the shear reinforcing effectiveness of PP-ECC.

Fig. 22 shows the stiffness degradation of all specimens during the cyclic loading, which was assessed by computing the slope of the line connecting the peak load and zero load at half cycle of each drift level. Even with the elimination of transverse reinforcements in TJ-2 and TJ-3, TJ-2 and TJ-3 exhibited the comparable performance of TJ-1, indicating that the little effect on the stiffness degradation due to the reduction of transverse reinforcements by using PP-ECC. In addition, it was noted that although the crushing of the defective PP-ECC on the view side in TJ-3 was observed during the loading tests, the comparable energy dissipation and stiffness degradation exhibited by TJ-3 indicates that the effect resulting from this defective PP-ECC was ignorable.

Table 7
Summary of experimental results.

	TJ-1	TJ-2	TJ-3
First cracking drift cycle	0.5% – 1st	0.5% – 1st	0.5% – 1st
Load at the peak when positive loading	23.4 kN	21.1 kN	19.6 kN
Load at the peak when negative loading	18.0 kN	17.2 kN	18.6 kN
Total horizontal joint shear force (V_{jh})	138.9 kN	125.3 kN	116.4 kN
Peak joint shear stress (v_j)	2.2 MPa	2.0 MPa	1.9 MPa
Ratio of peak joint shear stress to $\sqrt{f'_c}$	0.32	0.35	0.32
Pull out of longitudinal reinforcements in beam	Top reinforcements	Bottom reinforcements	No
Beam reinforcements rupture	5 out of 14	2 out of 14	6 out of 14
Failure mode	Flexural	Flexural	Flexural

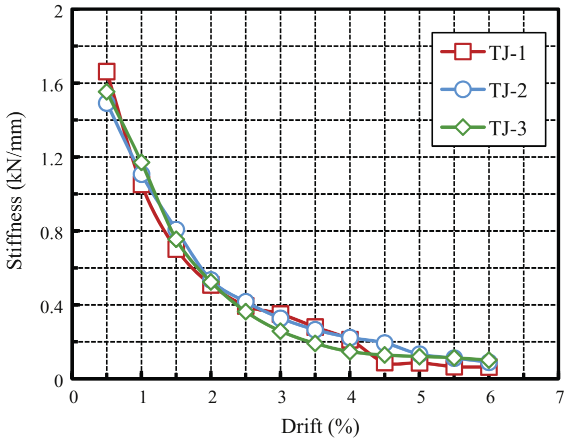

(a) Positive loading.

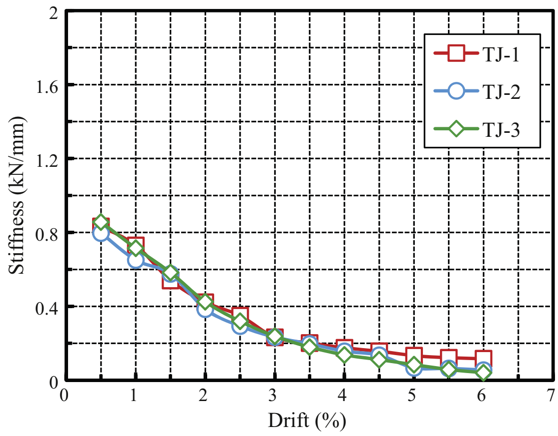

(b) Negative loading.

Fig. 22. Stiffness degradation.

6. Conclusions

The four-point bending experiments of the beams with reduced stirrups were conducted to investigate the shear behavior of PP-ECC beams. Then the reverse cyclic loading tests were performed to eliminate the transverse reinforcements in the beam–column joint connections of railway rigid-framed bridges which were designed following the Japanese railway design code. The present study indicates that PP-ECC is a possible alternative to replace the transverse reinforcements to provide the sufficient ductility thereby strikes a balance between economy and workability in beam–column joint connections of railway rigid-framed bridges. Based on the experimental results, the following conclusions can be drawn:

1. At the $a/d = 2.8$, the shear capacity of the beams with and without stirrups increases 20.6% and 107.6%, respectively by replacing concrete with PP-ECC. It also appears feasibility that the PP-ECC could be a replacement of the transverse reinforcement in beam–column joint connection specimens.
2. The reduction of transverse reinforcements in the beam, the column and the joint improved the workability and increased economy of using PP-ECC.
3. The failure mode of the specimens even with elimination of transverse reinforcements was still flexural failure, which was the same as that of the specimen without elimination of transverse reinforcements indicating that the PP-ECC can be the replacement of transverse reinforcements to provide sufficient shear strength.
4. The peak loads of PP-ECC joint specimens with elimination of transverse reinforcements remained comparable to the specimen without elimination of stirrups in the beam without shear failure, indicating that the PP-ECC can act as transverse reinforcements to carry the applied load.
5. Sufficient ductile behavior could be achieved even with reduction of the transverse reinforcements by using PP-ECC.
6. The specimens with the reduction of transverse reinforcements by using PP-ECC dissipated more energy than that without elimination of transverse reinforcements.

Acknowledgement

The authors are grateful to Dr. Kabir Shakya of the Chiyoda Corporation for his precious suggestions in this study.

References

[1] Tang J, Hu C, Yang K, Yan Y. Seismic behavior and shear strength of framed joint using steel-fiber reinforced concrete. ASCE J Struct Eng 1992;118(2):341–58.
[2] Filiatrault A, Ladicani K, Massicotte B. Seismic performance of code-designed fiber-reinforced concrete joints. ACI Struct J 1994;91(5):564–70.
[3] Filiatrault A, Pineau S, Houde J. Seismic behavior of steel-fiber reinforced concrete interior beam–column joints. ACI Struct J 1995;92(5):1–10.
[4] Bayasi Z, Gebman M. Reduction of lateral reinforcement in seismic beam–column connection via application of steel fibers. ACI Struct J 2002;99(6):772–8.
[5] Shakya K, Watanabe K, Matsumoto K, Niwa J. Application of steel fibers in beam–column joints of rigid-framed railway bridges to reduce longitudinal and shear rebars. Constr Build Mater 2012;27(1):482–9.
[6] Abbas AA, Mohsin SMS, Cotsovos DM. Seismic response of steel fibre reinforced concrete beam–column joints. Eng Struct 2014;59:261–83.
[7] Li V. In: Banthia N, Mufti A, editors. Engineered Cementitious Composites (ECC) – tailored composites through micromechanical modeling, fiber reinforced concrete: present and the future. Canadian Society of Civil Engineers; 1998. p. 64–97.
[8] Li V, Fischer G. Effect of matrix ductility on deformation behavior of steel reinforced ECC flexural members under reversed cyclic loading conditions. ACI Struct J 2002;99(6):781–90.
[9] Parra-Montesinos G, Peterfreund S, Chao S. Highly damage-tolerant beam–column joints through use of high-performance fiber-reinforced cement composites. ACI Struct J 2005;102(3):487–95.
[10] Qudah S, Maalej M. Application of Engineered Cementitious Composites (ECC) in interior beam–column connections for enhanced seismic resistance. Eng Struct 2014;69:235–45.
[11] Hirata T, Kawanishi T, Okano M, Watanabe S. Study on material properties and structural performance of high-performance cement composites using polypropylene fiber. Proc Jpn Concr Inst 2009;31(1):289–94 [in Japanese].
[12] Brown R, Shukla A, Natarajan KR. Fiber reinforcement of concrete structures. University of Rhode Island Transportation Center (URITC) Project No. 536101; 2002.
[13] Railway Technical Research Institute. Design standards for railway structures and commentary (concrete structures); 2004.
[14] Japan Society of Civil Engineers (JSCE). Standard specifications for concrete structures-2007 (structural performance verification); 2010.
[15] Japan Society of Civil Engineers (JSCE). Standard specifications for concrete structures-2007 (materials and construction); 2010.
[16] Okano M, Watanabe K, Hirata T, Kawanishi T. Basic structural performance of HPFRCC using polypropylene fibers. In: 63th Japan Society of Civil Engineers annual meeting; 2008. p. 1061–2 [in Japanese].
[17] ACI Committee 318. Building code requirements for structural concrete (ACI 318-11); 2011.
[18] Joint ACI-ASCE Committee 352. Recommendations for design of beam–column connections in monolithic reinforced concrete structures; 2002.
[19] Kojima S, Sakata N, Kanda T, Hiraishi T. Retrofitting application of spraying high ductile cementitious composites. JCI Concr J 2004;42(5):135–9 [in Japanese].